Dendrimers in Biomedical Applications

Dendrimers in Biomedical Applications

Edited by

Barbara Klajnert
University of Lodz, Poland

Ling Peng
Centre Interdisciplinaire de Nanoscience de Marseille, France
Email: ling.peng@univmed.fr

Valentín Ceña
Universidad de Castilla-La Mancha, Albacete, Spain

RSC Publishing

This work is a publication of the COST Action Group TD0802

ISBN: 978-1-84973-611-4

A catalogue record for this book is available from the British Library

Published by The Royal Society of Chemistry,
Thomas Graham House, Science Park, Milton Road,
Cambridge CB4 0WF, UK

Registered Charity Number 207890

Visit our website at www.rsc.org/books

ESF provides the COST Office through an EC contract

COST is supported by the EU RTD Framework programme

COST – the acronym for European Cooperation in Science and Technology- is the oldest and widest European intergovernmental network for cooperation in research. Established by the Ministerial Conference in November 1971, COST is presently used by the scientific communities of 36 European countries to cooperate in common research projects supported by national funds.

The funds provided by COST - less than 1% of the total value of the projects - support the COST cooperation networks (COST Actions) through which, with EUR 30 million per year, more than 30 000 European scientists are involved in research having a total value which exceeds EUR 2 billion per year. This is the financial worth of the European added value which COST achieves.

A "bottom up approach" (the initiative of launching a COST Action comes from the European scientists themselves), "à la carte participation" (only countries interested in the Action participate), "equality of access" (participation is open also to the scientific communities of countries not belonging to the European Union) and "flexible structure" (easy implementation and light management of the research initiatives) are the main characteristics of COST.

As precursor of advanced multidisciplinary research COST has a very important role for the realisation of the European Research Area (ERA) anticipating and complementing the activities of the Framework Programmes, constituting a "bridge" towards the scientific communities of emerging countries, increasing the mobility of researchers across Europe and fostering the establishment of "Networks of Excellence" in many key scientific domains such as: Biomedicine and Molecular Biosciences; Food and Agriculture; Forests, their Products and Services; Materials, Physical and Nanosciences; Chemistry and Molecular Sciences and Technologies; Earth System Science and Environmental Management; Information and Communication Technologies; Transport and Urban Development; Individuals, Societies, Cultures and Health. It covers basic and more applied research and also addresses issues of pre-normative nature or of societal importance. For more information the web address is: http://www.cost.eu

This publication is supported by COST.

PREFACE

Dendrimers are a special class of polymers with a well-defined structure and intriguing architecture bearing unique radiating branching units in the interior and numerous end groups on the surface. Unlike traditional polymers, the structures of dendrimers can be precisely controlled during their stepwise synthesis, yielding narrow polydispersity in addition to unique structural geometry and multivalent properties. Consequently, dendrimers are particularly appealing for biomedical applications. However, there is still a substantial gap in understanding how dendrimers act, and the pace of translating research from bench to bedside is far from satisfactory. It requires joint efforts from scientists with backgrounds including chemical synthesis, physical characterization, biological evaluation and clinical design. Along these lines, COST Action TD0802 "Biomedical applications of dendrimers" was established in 2008 to build a multidisciplinary European network. Its goal has been to establish a network of collaborative European research aimed at developing new medical applications based on dendrimer technology by making full use of the unique properties of dendrimers. The fruitful results of this Action have relied on its highly interdisciplinary approach in which chemists, physicists, biologists and physicians have all been involved in the collaboration. This effort has also clearly shown that it is possible to establish a successful network of cooperating research groups in a short time in Europe, which can be further continued on a long-term basis.

This book presents an overview of the-state-of-the-art in the field of dendrimer research and its biological applications. The chapters cover various aspects from the synthesis and characterization of different types of dendrimers such as polyaminoester dendrimers and multivalent dendrons (chapters 9, 12 and 13); characterization of dendrimer-based hybrid nanofibers as potential templates for 1D-objects (chapter 2); the use of different families of dendrimers for biomedical applications such as drug and genetic material delivery (chapters 3 to 6 and 10); antiamyloidogenic effects (chapter 1); anti-inflammatory actions (chapter 5) and dendrimers as sensors for drug allergy detection (chapter 7). In addition, several chapters discuss the use of molecular modeling to investigate the interaction of dendrimers with biological molecules (chapters 2, 4, 6, 8, 10 and 11).

Overall, this book can be useful for both newcomers to the field by presenting an overview of the research being performed in the field, and to the researchers working on dendrimers by presenting in-depth studies on various aspects of dendrimer synthesis and applications. We hope that more and more scientists will join the interdisciplinary research on dendrimers and make their contribution to the fast growing and fascinating world of dendrimers.

Valentin Ceña

Barbara Klajnert

Ling Peng

Contents

MULTISCALE MODELING OF DENDRIMERS AND DENDRONS FOR DRUG AND NUCLEIC ACID DELIVERY

P. Posocco,[1] E. Laurini,[1] V. Dal Col,[1] D. Marson,[1] L. Peng,[2] D.K. Smith,[3] B. Klajnert,[4] M. Bryszewska,[4] A.-M. Caminade,[5] J.P. Majoral,[5] M. Fermeglia,[1] K. Karatasos[6] and S. Pricl[1]

[1]Molecular Simulation Engineering (MOSE) Laboratory, DEA, University of Trieste, Piazzale Europa 1, 34127 Trieste, Italy
[2]Centre Interdisciplinaire de Nanoscience de Marseille, CNRS UMR 7325, 163, avenue de Luminy, 13288 Marseille, France
[3]Department of Chemistry, University of York, Heslington, York, YO10 5DD, United Kingdom
[4]Department of General Biophysics, University of Lodz, Pomorska st. 141/143, Lodz 90-236, Poland
[5]Laboratorie de Chimie de Coordination, CNRS, UPR 8241 205, route de Narbonne 31077, Toulouse, France
[6]Chemical Engineering Department, Aristotle University of Thessaloniki, University Campus, 54124, Thessaloniki, Greece

1 INTRODUCTION

Multiscale molecular simulations of drug delivery systems (DDSs) is poised to provide predictive capabilities for the rational design of targeted DDSs, including multi-functional nanoparticles such as dendrimers and dendrons as highly specialized delivery nanovectors. Realistic three-dimensional atomistic and mesoscopic models can provide a framework for understanding the fundamental physico-chemical interactions between the active principles, their nanocarriers and, ultimately, the patient physiology. The wide range of emerging nanotechnology systems for targeted delivery further increases the need for reliable *in silico* predictions.

Multiscale modeling, however, is in its infancy even for conventional drug delivery. The projection that by 2016 about 30% of pharmaceutical R&D expenditure will be on computer simulation connote that we will see more and more sophisticated molecular models developed. Due to the permutations of the confounding factors that complicate the traditional experimental (wet lab) approach, the need for multiscale computational models is even higher for the design of drug delivery systems of nanoparticles that involve multiscale processes both in the spatial and temporal dimensions. Thus, a pathway to future designs of smart delivery systems will be integration of the different elements at various levels of scales involving the physico-chemical and biological phenomena, as shown in Figure 1.

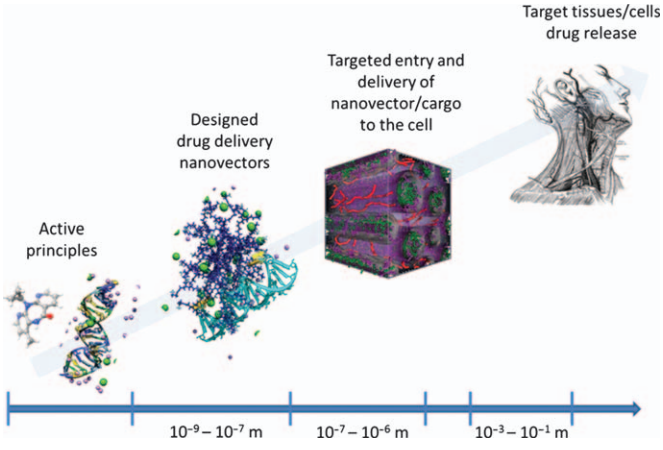

Figure 1 *The (multi)length scale of a nanovector-assisted drug delivery process.*

In recent years, the use of computer simulations as a tool for bridging between microscopic length and time scales and the macroscopic world of the laboratory has been increasing exponentially. The main reasons for this success is that, by using computational chemistry and physics, a guess at the interactions between molecules can be provided, and `exact' predictions of bulk properties can be obtained. The predictions are `exact' in the sense that they can be made as accurate as we like, subject to the limitations imposed by the available computer budget. At the same time, the hidden detail behind bulk measurements can be revealed. Simulations act as a bridge in another sense: between theory and experiment. A theory can be tested by conducting a simulation using the same model. The model can be tested by comparing with experimental results. Also, simulations can be carried out on the computer that are difficult or impossible in the laboratory (for example, working at extremes of temperature or pressure).

The actual computational modeling of biological macromolecules, mainly based on molecular dynamics (MD) simulations, commonly revolves around structure representations in atomic or near-atomic detail, with a classical description of physical interactions. In a typical MD simulation, the atomic trajectories of a system of N (e.g., 10^6) particles are generated by numerical integration of Newton's equation of motion, for a specific interatomic potential, with certain initial and boundary conditions. Such models have been quite successful in complementing experimental data with structural, dynamic, and energetic information, but involve substantial computational resources for larger systems, or when long time scales have to be considered. In particular, structure-activity calculation applications, the formation and interaction of supramolecular assemblies, and the prediction of kinetic and transport phenomena will necessarily involve extremely extensive computational resources when using models at atomic details, if they are feasible at all.

Thus, we are also in the need of developing some computational strategy to link the atomic length and time scales of MD to the macroscopic length and time scales (nanometers to micrometers and nanoseconds to microseconds): the so-called *mesoscale* phase. Only by establishing this connection from nanoscale to mesoscale it is possible to build first principles methods for describing the properties of new materials and systems for biomedical and life science applications, of which RNA/DNA delivery systems are prototypical examples.[1]

This linking through the mesoscale in which the microstructure can be described over a length scale of tens to hundred nanometers is probably the greatest challenge to develop reliable first principles method for practical material design applications. Scale integration in specific contexts in the field of (bio)macromolecular modeling can be done in different ways. Any *recipe* for passing information from one scale to another (upper) scale is based on the proper definition of many-scale modeling which considers *objects* that are relevant at that particular scale, disregards all degrees of freedom of smaller scales, and summarizes those degrees of freedom by some representative parameters (see Figure 2).[2]

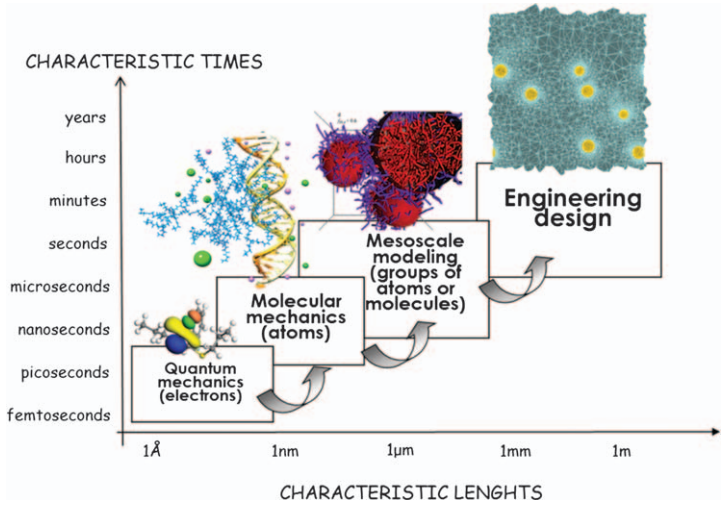

Figure 2 *The multiscale molecular modeling concept: the information obtained from simulations at a given (lower) characteristic length and time scales is used as an input for the next (upper) scale simulations.*

Under the multiscale molecular modeling perspective outlined above, the current ambitious aim of our research group is to reach the domain of nucleic acid delivery system engineering by building from fundamental principles of physics and chemistry. Hence, for fundamental predictions to play a direct role in these materials innovation and design, it is mandatory to bridge the micro-macro gap, thus establishing a tight and direct coupling between *in silico* and *in vitro*/*in vivo* experiments.

2 STUCTURAL CHARACTERIZATION OF DENDRONS AND DENDRIMERS

Dendrimers (or any other macromolecule) entering the systemic circulation distribute to tissues largely via the bloodstream. Therefore, the blood flow rate determines the delivery rate of macromolecules to each tissue. Dendrimers in the circulation have direct access to the capillary endothelial cells, as well as various circulating cells in the blood. These cells have the opportunity to take up the macromolecules via specific or non-specific interactions. The interaction of macromolecules with parenchymal cells in tissues can occur only when they have access through the endothelial lining.

The structure of the blood capillary walls varies greatly depending on the organ. In addition, pathological states such as inflammation could change the structure. On the basis of the morphology and continuity of the endothelial layer and the basement membrane, the capillary endothelium can be divided into continuous, fenestrated, and discontinuous endothelium. Tight junctions between endothelial cells and underlying uninterrupted basement membrane characterize the continuous endothelium, through which the passage of polymeric molecules is greatly hampered. Such type of endothelium characterizes the

skeletal, cardiac, and smooth muscles, and can be found in lung, skin, and subcutaneous tissues. Dendrimeric and other polymer-based nanoparticles with diameters equal or greater than 6 nm hardly interact with parenchymal cells in these tissues, simply because of the barriers posed by the endothelium. Endothelial cells having fenestrae featuring a diaphragm - an opening 40-80 nm in diameter – form the fenestrated endothelium found in the intestinal mucosa, the endocrine and exocrine glands, and the gromerulus and peritubules of the kidney. However, the passage of macromolecules through this type of endothelium is limited by the presence of the basement membrane. The discontinuous (or sinusoidal) endothelium is found only in the liver, spleen, and bone marrow. These capillaries are characterized by endothelial gaps, intracellular junctions with a diameter up to 30-500 nm and with either no basement membrane (liver) or a discontinuous basement membrane (spleen and bone marrow). Therefore, parenchymal cells in these tissues can be accessed by macromolecules with relatively high molecular weight and, consequently, large dimensions. A similar situation (i.e., big fenestrations and enhanced vascular permeability of nanoparticle-based drug delivery systems) are also found in several solid tumours.

According to the above discussion the size and, hence, the structure of dendrimers as a function of pH is a critical issue for their utilization as drug delivery vehicles in physiological environments (pH = 7.4). Molecular simulations can provide insights into the structure and the properties of dendrimers as a function of generation by yielding, for instance out of a plethora of many others, the values of the radius of gyration R_g and the corresponding radial distribution functions of the dendrimers via fully atomistic MD simulations in explicit solvent, counterions, and ionic strength.

2.1 Dimensions and Shape of Viologen Dendrimers

Viologen-phosphorus containing dendrimers are relatively new compounds which have been seldom investigated in terms of their biological and, even less, of their structural properties.[3] These types of compounds exhibit antimicrobial properties and their behavior depends on their size, the number of viologen units and the nature of the surface groups.[3(a),4]. Quite recently, Erik De Clercq and collaborators[5] proved the antiviral activity of dendrimers containing a viologen against the Human Immunodeficiency Virus (HIV), and, to a lesser extent, against other viruses such as the Herpes Simplex Virus (HSV), the Reovirus (RV), and the Respiratory Syncytial Virus (RSV).

Accordingly, we embarked in a complex computational study to determine the main structural characteristics of some representative members of the viologen-based dendrimers, and their binding to albumin.[4] In particular, we focused on two different families of new viologen dendrimers bearing phosphorus groups as additional units incorporated either at the focal point or at the periphery or both of these key structural positions of the dendritic backbone.[3] This choice of strategy was aimed by the fact that we already demonstrated the key role played by phosphorus dendrimers in biology and for biomedical applications due to several specificities.[6]

Accordingly, the two viologen-phosphorus dendrimers were built from a trifunctionalized core $P(S)(NCH_3NH_2)_3$ (**D2**, **D4**, and **D6**) or from a hexafunctionalized core $(P_3N_3)(NCH_3NH_2)_6$ (**D3**, **D5**, and **D7**), and decorated on their surface either with aldehyde groups or with phosphonate groups, the latter being well-known for their biological properties. A dendron structurally similar to **D2** but stemming from a phenyl core (**D1**) was also considered for comparison.

Scheme 1 illustrates the chemical structures of the viologen dendrimers **D1**-**D7**, while Figure 3 shows the MD equilibrated snapshots of **D4** and **D7** at neutral pH and in the presence of a physiological ionic strength (0.15 M) in solution.

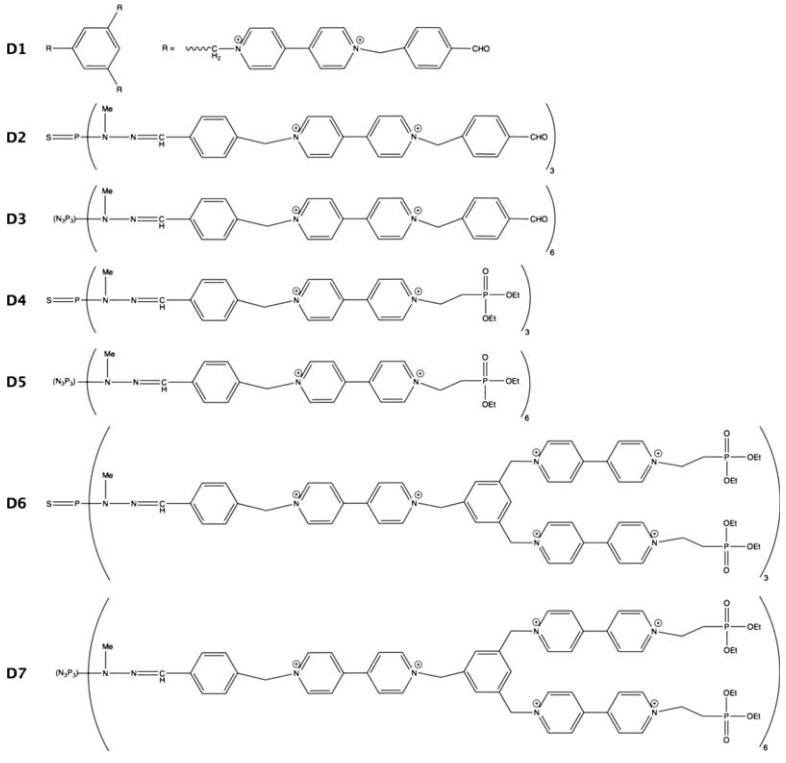

Scheme 1 *Chemical structures of the viologen dendrimers **D1**-**D7**.*

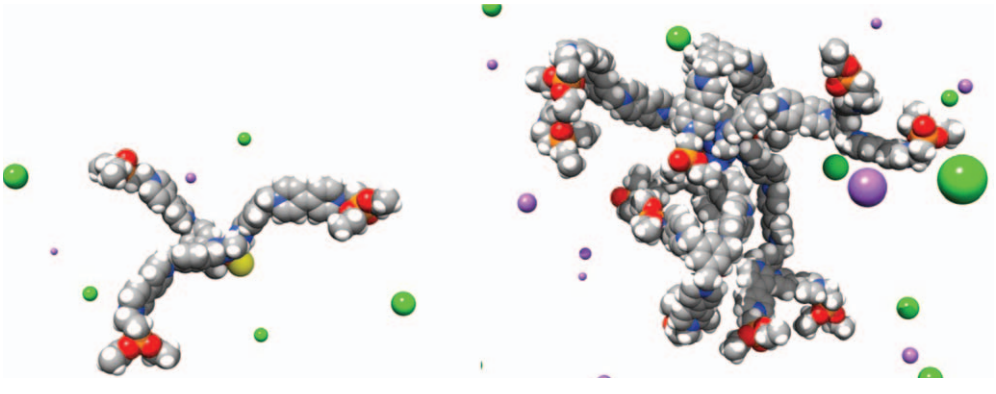

Figure 3 *Equilibrated MD snapshots of viologen-phosphorous **D4** (left) and **D7** (right) in solution at neutral pH and 0.15 M NaCl. The dendrimers are shown as atom-coloured spheres (grey, C; red, O; yellow, S; blue, N, orange, P, white, H). Water molecules are omitted for clarity, while some counterions are shown as green (Cl^-) and purple (Na^+) spheres.*

The radius of gyration R_g is a fundamental tool for the description of structural properties of dendrimeric molecules and other macromolecules as well. This quantity, related to the square root of the second invariant of the first order tensor ***S***, takes into

account the spatial distribution of the atom chain by mediating over all N molecular components. For a dendrimer, the mean-square radius of gyration is defined by:

$$R_g^2 = \frac{1}{M_w}\langle \sum_{i=1}^{N} m_i \, |\boldsymbol{r}_i - \boldsymbol{R}|^2 \rangle \quad (1)$$

where $\boldsymbol{R}$ is the centre of mass of the dendrimer, $\boldsymbol{r}_i$ and m_i are the position and mass of the i^{th} atom, and M_w refers to the total mass of the dendrimer. The R_g values estimated by MD simulations for all viologen dendrimer generations $\boldsymbol{G}$ at pH = 7.4 and 0.15 M NaCl are listed in the fourth column of Table 1. As shown in Figure 4A, the dimensions of the viologen dendrimers linearly increase with increasing generation $\boldsymbol{G}$.

Table 1 *Main Structural Parameters for Viologen Dendrimers **D1-D7***

Dendrimer	Charge	G	R_g (Å)	Asphericity
D1	+6	0	9.25	0.078
D2	+6	0	10.76	0.063
D3	+12	0	12.32	0.020
D4	+6	0	12.19	0.081
D5	+12	0	13.07	0.023
D6	+18	1	16.59	0.069
D7	+36	1	18.82	0.026

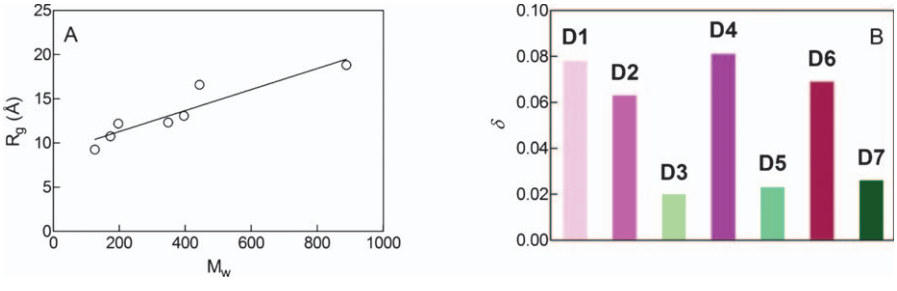

Figure 4 *(A) Plot of R_g calculated from MD simulations as a function of the viologen dendrimers molecular weight at pH = 7.4 and 0.15 M NaCl. (B) Plot of the asphericity parameter δ for all viologen dendrimers.*

While the value of R_g, yields an indication of the overall dimension of the dendrimers, it does not inform about the real shape of the molecules, that is, if the dendrimer is adopting a true spherical or, e.g., an oblong shape. To check this, MD data can be further exploited to characterize the shape of the dendrimers by calculating the molecular asphericity parameter as:

$$\delta = 1 - 3\,\langle I_2 \rangle / \langle I_1^2 \rangle \quad (2)$$

where I_1 and I_2 are the first two invariants of the radius of gyration tensor $\boldsymbol{S}$. By definition, the asphericity parameter can take values ranging from 0 (i.e., a sphere) to 1 (a line). The fifth column of Table 1 and the graph in Figure 4B show that all viologen dendrimers tend to assume a spherical conformation; nonetheless, the dendrimers featuring the cyclotriphosphazene moiety as a core (**D3**, **D5**, and **D7**) and characterized by 6 branches all present a δ value close to 0.02 and, thus, assume a more spherical than their 3-branched trihydrazidophosphine-core or phenyl-core counterparts (**D1**, **D2**, **D4**, and **D6**). Such a behaviour can be ascribed to the presence of regularly spaced like-charges along the

dendrimer branches, whose reciprocal repulsion (greater for those molecules with a higher number of ramifications) finds a global equilibrium condition in the adoption of a more regular and spherical shape.

2.2 Flexibility and Back-Folding of PAMAM-like Dendrimers

2.1.1 TEA-core PAMAM dendrimers as highly flexibly nanocarriers. Recently, Peng et al. showed that PAMAM dendrimers based on a triethanolamine (TEA) core (see Scheme 2) are effective vectors for siRNA delivery and gene silencing using both a luciferase model[7] and a functional siRNA to target the heat shock protein 27 in castrate-resistant prostate cancer.[8]

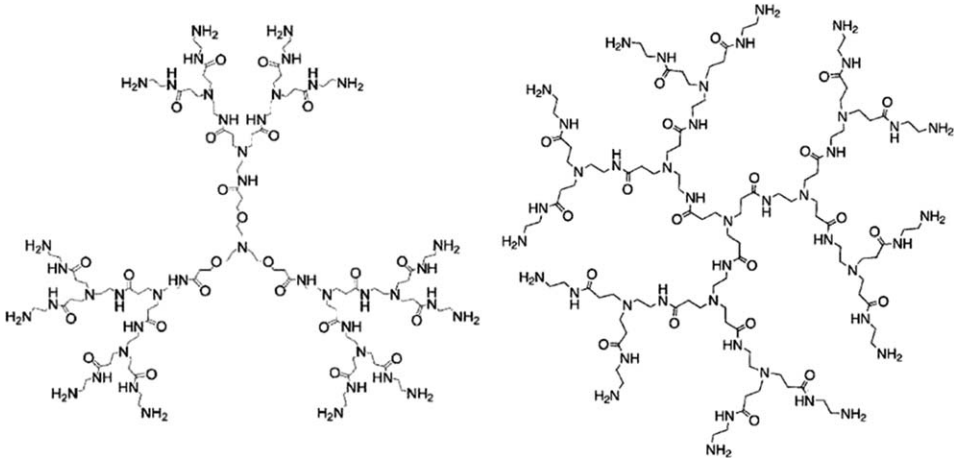

Scheme 2 *Chemical details of the TEA-core (left) and NH_3-core PAMAM dendrimers. For clarity, dendrimers of the second generation (G_2) are shown.*

The rationale behind the synthesis of this new dendrimer family was that the TEA-core dendrimers, having the branching units starting away from the central amine with a distance of 10 successive bonds, should feature an extended core, and are expected to be less congested in space with respect to the prototypical NH_3-core PAMAM dendrimers, for which the branches sprout directly from the small ammonia focal point. Consequently, the TEA-core dendrimers, with their branching units and terminal end groups being less densely packed than those of NH_3-core dendrimers, should be endowed with an enhanced flexibility of their arms if compared to more congested dendrimeric families and, as such, able to perform better as *e.g.*, DNA or siRNA nanocarriers. Indeed, a larger flexibility should in principle allow a nanocarrier to *i*) more effectively enwrap its genetic material and *ii*) act as a better more efficient proton sponge.

Accordingly, information on the structural diversity between TEA-core and NH_3-core based PAMAM dendrimers were obtained by applying atomistic MD simulations.[9,10] As an example, Figure 5A and 5B shows two equilibrium MD snapshots of the generation 5 dendrimers of the TEA-core (***G*$_5$**) and the NH_3-core (***G*$_5$'**) PAMAM dendrimers at neutral pH, respectively. The structural difference which characterizes these two macromolecules is apparent at first glance: whilst ***G*$_5$** has a more open conformation featuring uniform void spacing in its interior, the ***G*$_5$'** counterpart is more compact, with its monomer units distributed more uniformly within the entire molecule and a non-homogeneous, restricted void spacing (Figure 5A). Accordingly, the conformation of the TEA-core dendrimer ***G*$_5$** is such that the outer branches can readily move and adjust for optimizing an ultimate

binding with its nucleic acid cargo. On the contrary, in the case of the NH_3-core dendrimer ***G5'***, its more rigid and compact structure prevents this molecule for any *induced-fit* conformational readjustment and, consequently, not all terminal amine groups are available to self-orient for optimal cargo binding (see Figure 5B).

A quantitative support to this pictorial view can be obtained by considering the average radial monomer density $\rho(r)$, a quantity defined as the number of atoms whose centres of mass are located within a spherical shell of radius r and thickness Δr. Integration over r yields the total number of monomers as:

$$N(r) = 4\pi \int_0^R r^2 \rho(r) dr \tag{3}$$

Figure 5C and 5D shows the radial monomer density profiles for the TEA-core ***G5*** and the NH_3-core ***G5'*** dendrimer molecules, respectively. In each case, the plot shows the contribution to the particular generation from each of its component generations. In each case, the molecular centre of mass was taken as the origin. When considering ***G5***, the whole dendrimer $\rho(r)$ curve (thick continuous line in Figure 5C) shows a minimum around 10 Å away from the core, and another, smaller minimum at approximately 17 Å. These, together with the two relative maxima (located at ~ 13 and 21 Å), indicate that *i*) the core region becomes denser compared with the middle of the dendrimer, which is fairly hollow, and *ii*) the higher sub-generation monomers form a crowded layer at the dendrimer periphery. This is perfectly matching the portray of the molecule as resulting from the snapshot of the MD simulations (Figure 5A). Further, from Figure 5C we can see that this increase in density at the core stems only from the density of the inner generations. The outermost generations do not contribute to this density, but contribute mainly to the density of the outmost layers. Because of the presence of uniform, hollow spaces in the inner/middle regions of the dendrimer, a significant number of water molecules are able to penetrate to the molecular middle region, as depicted by the corresponding thick dashed curve in Figure 5C. Considering now ***G5'***, the corresponding profile of the $\rho(r)$ curve for the whole dendrimer is pretty different (see Figure 5D). Starting form the core peak, we see a uniform decrease and then a plateau value in the monomer density all across the molecular structure, followed by a secondary peak, again at the molecular periphery. Accordingly, all sub-generations contribute substantially to the whole density curve, pointing to a more uniform monomer distribution inside the dendrimer molecule (see also Figure 5B). In harmony with this evidences, water does not show a pronounced maximum in any specific region of the molecule but is also uniformly distributed within the molecular interior (thick dashed curve in Figure 5D).

2.1.2 Back-folding of PAMAM dendrimers. A further, peculiar feature of dendrimeric structures which may affect their performance as nanocarriers is the high degree of back-folding. The usual schematic diagrams found in the literature for dendrimers, particularly the 2D representations, convey the idea that the terminal groups are located at the periphery of the molecule. However, actual MD simulations reveal the presence of a substantial back-folding of the end groups toward the dendrimer core.[10,11] To quantify this aspect, the radial distribution functions for terminal nitrogen atoms for various generations of the "gold standard" diethylenediamine (DEA) PAMAMs are reported in Figure 6A and 6B.

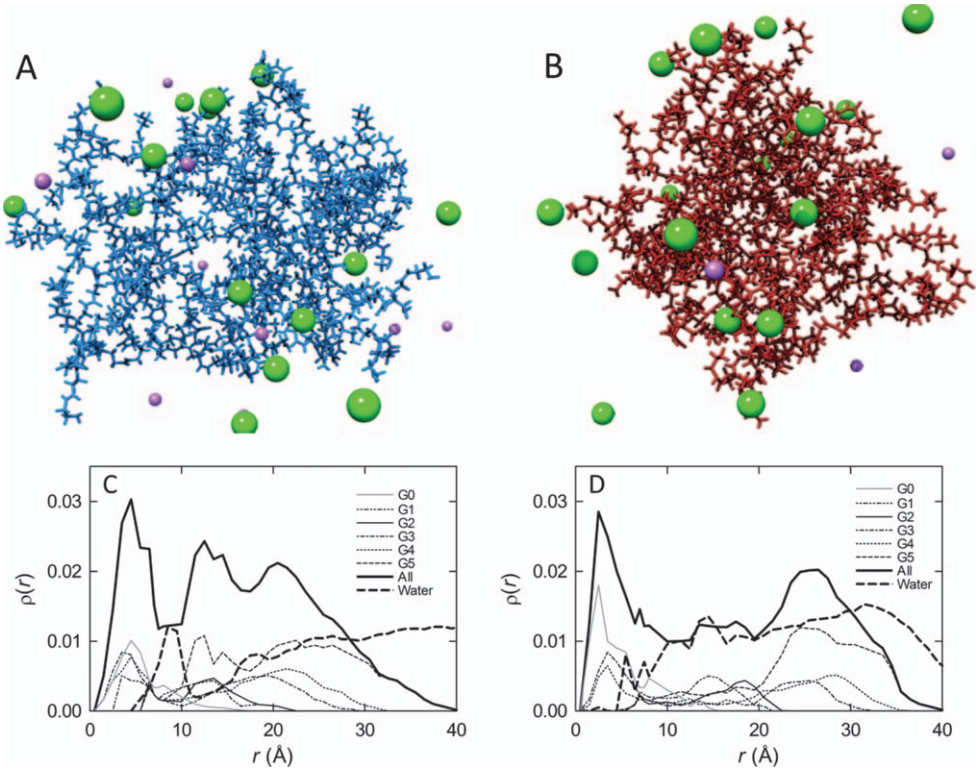

Figure 5 *Top panels: snapshots of typical equilibrium configurations of G5 (A) and G5' (B) dendrimers at pH = 7.4 and 0.15 M NaCl. Dendrimers are shown as coloured sticks, while some counterions are portrayed as green (Cl^-) and purple (Na^+) spheres. Water is not shown for clarity. Bottom panels: radial monomer density profiles for TEA-core dendrimer* $\mathbf{G_5}$ *(C) and* NH_3*-core dendrimer* $\mathbf{G_5'}$ *(D).*

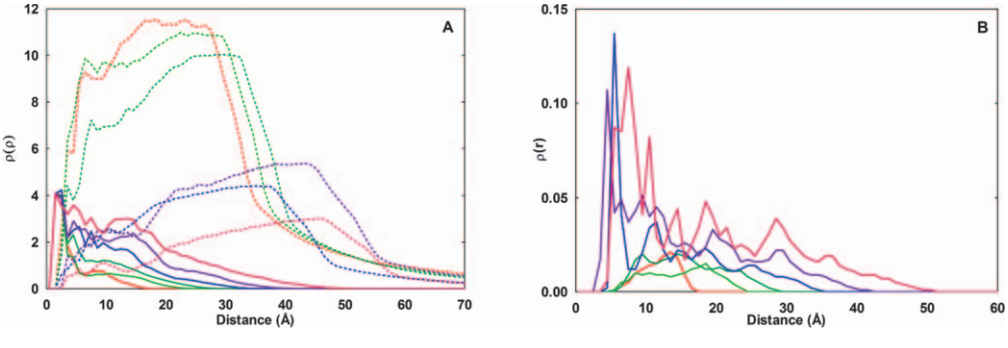

Figure 6 *(A) Radial density distributions for PAMAM generations* $\mathbf{G_1}$ *to* $\mathbf{G_6}$ *(continuous lines) and water (broken lines) at pH = 7.4. (B) Radial density distributions for terminal nitrogen atoms of PAMAM generations* $\mathbf{G_1}$ *to* $\mathbf{G_6}$ *at pH = 7.4. Colour legend: red,* $\mathbf{G_1}$*; light green,* $\mathbf{G_2}$*; dark green,* $\mathbf{G_3}$*; blue,* $\mathbf{G_4}$*; purple,* $\mathbf{G_5}$*; dark red,* $\mathbf{G_6}$*. Adapted from PAMAM dendrimers for siRNA delivery: computational and experimental insights, Pavan, G.M.; Posocco, P.; Tagliabue, A.; Maly, M.; Malek, A.; Danani, A.; Ragg, E.; Catapano, C.V.; Pricl, S. Chemistry Eur. J. 16(26), Copyright © [2010], John Wiley & Sons, http://onlinelibrary.wiley.com/doi/10.1002/chem.200903258/pdf.*

These distributions reveal that the dendrimer end groups are sufficiently flexible to interpenetrate nearly the whole molecule. In particular, the end groups of higher

generations come even close to the core of the molecule, and the extent of back-folding increases with increasing dendrimer generation ***G***. This effect is more evident at neutral pH; higher generations show pronounced peaks near the core of the molecule and, for smaller generations, the back-folding pervades the entire molecular architecture. Obviously, the presence of a substantial back-folding is detrimental to nucleic acid binding, as less protonated terminal groups are available on the dendrimer surface; accordingly, the overall dendrimer surface charge is diminished, the corresponding ionic interactions with the genetic material is lower, and the nucleic acid cargo might be lost along the way to the target cell under the action of drag forces in the blood stream or the uptake of plasma proteins. On the other hand, a too strong interaction between the nanovector and its cargo can turn out to be unfavourable in a later stage of the delivery process, that is during cargo release in the cell cytoplasm: a tight electrostatic bond between the two molecular entities may disfavour the nucleic acid detachment from its vector, thus making the genetic material unavailable for further, therapeutic action.

3 BINDING OF DENDRON/DENDRIMERS TO NUCLEC ACIDS

The ability of a nanocarrier to generate a stable complex with its nucleic acid payload is a background postulate for its usefulness in gene delivery. This property can be experimentally explored and quantified through the use of many disparate techniques, ranging from the standard Ethidium Bromide (EthBr) displacement fluorescence spectroscopy assay to the more sophisticate and quantitative isothermal titration calorimetry (ITC) or differential scanning calorimetry (DSC). Multiscale molecular simulations, however, not only can yield the same information in a less expensive way (both from time and money standpoint), but may offer a reliable molecular rationale to explain the generation, structural, ionic strength, and other chemico-physical properties and mechanisms determining the dependence of the affinity of a given dendrimer/dendron carrier to its nucleic acid cargo.[1,9-12]

Thus, in a recent study we demonstrated that the structurally flexible TEA-core poly(amidoamine) (PAMAM) dendrimers are excellent nonviral vectors for siRNA delivery both *in vitro* and *in vivo*.[8,9,13] Of particular interest, the generation 7 dendrimer ($\boldsymbol{G_7}$) can mediate efficient siRNA delivery and produce potent gene silencing of the heat shock protein 27 (Hsp27) leading to effective anticancer activity in a castration-resistant prostate cancer model.[8] Unfortunately, however, the large-scale synthesis of the good quality TEA-core dendrimer $\boldsymbol{G_7}$ is particularly challenging. This is due to the seemingly easy but rather time-consuming and meticulous control of the reaction conditions as well as the tedious procedures of purifying the resulting, high generation PAMAM dendrimers. Accordingly, the possibility of developing low generation dendrimers for the effective delivery of siRNA therapeutics constitutes *per se* a challenging but worthwhile goal.

Recently, Behr et al. discovered that siRNAs with short complementary A_n/T_n (n = 5 - 8) 3′ overhangs, named " sticky " siRNA could dramatically increase gene silencing efficiency when using polyethylenimine (PEI) as the delivery vector.[14] Given these premises, since the large-scale synthesis of good quality, high generation dendrimers is particularly challenging, we reasoned that, resorting to sticky siRNAs, it could be possible to achieve the same gene efficiency by exploiting lower generation dendrimers as nanovectors.

Indeed, we verified that TEA-core PAMAM dendrimers of generation 5 are able to deliver sticky siRNAs bearing complementary A_n/T_n with (n = 5 or 7) 3'overhangs efficiently to a prostate cancer model both in vitro and, most notably, in vivo, and produce potent gene silencing of the heat shock protein 27, leading to a notable anticancer effect.[15]

We further checked whether, in addition to the hypothesized formation of gene-like longer double strand RNA molecules, the two complementary A_n/T_n (n = 5 or 7) overhangs of the sticky siRNAs might also behave as a sort of protruding molecular arms, allowing the siRNA molecule to enwrap the spherical, low generation dendrimers with higher binding affinity compared with a conventional siRNA which has two short T_2/T_2 overhangs.

Therefore, we studied the complex formation of ***G5*** with different siRNA molecules (conventional siRNA with T_2/T_2 overhangs, and sticky siRNAs with either A_5/T_5 or A_7/T_7 overhangs) by atomistic MD techniques.[15] The *in silico* predicted affinities of each sticky siRNA and the ***G5*** dendrimer, as quantified by the corresponding free energy of binding ΔG_{bind}, reveal that the ΔG_{bind} values obtained for *G5* and the sticky siRNAs with A_5/T_5 or A_7/T_7 overhangs are lower (i.e., more negative and, hence, more favourable) than those calculated for ***G5*** and the conventional siRNA with T_2/T_2 overhangs (Table 3), which indicates that the binding affinity of ***G5*** for sticky siRNAs is higher than that of ***G5*** for conventional siRNA. Based on these results, we hypothesized that, in addition to the possible formation of gene-like longer double strand RNA molecules, stronger binding to dendrimer of sticky siRNAs over conventional siRNAs might also contribute to the enhanced delivery activity of ***G5***.

Table 2 *Free energy of binding between a TEA-core PAMAM dendrimer of generation 5 (**G5**) and a siRNA with T_2/T_2, A_5/T_5, and A_7/T_7 overhangs (conventional siRNA and sticky siRNAs), respectively. Adapted with permission from Liu, X.; Liu, C.; Laurini, E.; Posocco, P.; Pricl, S.; Qu, F.; Rocchi, P.; Peng, L. Efficient delivery of sticky siRNA and potent gene silencing in a prostate cancer model using a generation 5 triethanolamine-core PAMAM dendrimer. Mol. Pharm., 2012, 9, 470-481. Copyright {2012} American Chemical Society.*

System	ΔH_{bind} (kcal/mol)	$-T\Delta S_{bind}$ (kcal/mol)	ΔG_{bind} (kcal/mol)
G_5/siRNA (T_2/T_2 overhangs)	-571.1 ± 2.6	254.3 ± 4.3	-316.8 ± 5.0
G_5/sticky siRNA (A_5/T_5 overhangs)	-637.40 ± 2.8	250.0 ± 4.1	-387.4 ± 5.0
G_5/sticky siRNA (A_7/T_7 overhangs)	-690.2 ± 4.7	267.3 ± 5.3	-422.9 ± 7.1

4 SOLVATION OF DENDRIMER/NUCLEIC ACID COMPLEXES

Soft colloids and macromolecules with flexible structures and void pervading their entire complex molecular structure are necessarily hydrated not only in their outer shell. Indeed, ions and water can penetrate along the tortuous pathways of holes and channels of the macromolecular entity, eventually reaching down to the inner core. Upon binding of a dendrimer to a nucleic acid, water plays even more determining roles. First, it creates a bridge between the carrier and the DNA/RNA, by maintaining an hydration layer and ensuring the instauration of a hydrogen bond network between the carrier and the nucleic acid, critical to their complex formation and stability. More important, perhaps, is the role of overall solubilization. Water and the solution navigating salts must pervade the entire system to guarantee uniform hydration and dispersion of the loaded nanoparticles, avoiding their aggregation and collapse.

Mesoscale simulations offer the possibility to predict and study this type of behaviour; in fact, a typical result of a mesoscale simulation is the morphology and the structure of matter at nanoscale level at the desired environmental conditions.[2,9] Let us then consider Figure 7, where the nanoscale morphology of a DNA/***G6*** complexes of TEA-core dendrimer (see §2.2.1 and §3) is presented. As it can be seen from this Figure, the TEA dendrimers are able to complex the DNA strands efficiently and homogeneously, with the DNA chains well enwrapped in the systems and the absence of DNA bundles at the nanoscopic level. Further, the water density maps at the mesoscopic level not only support the lower-scale (i.e., atomistic MD) results discussed above of a higher degree of hydration

but also confirm the uniform water molecule distribution within the nucleic acid/TEA-core PAMAM dendrimer.

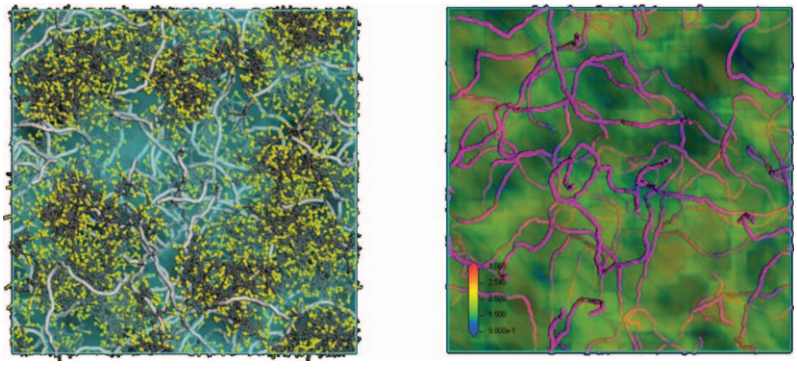

Figure 7 *(Left) Mesoscale morphologies of the assembled systems between TEA-core dendrimers* $\boldsymbol{G_6}$ *and DNA. The dendrimers are represented as dark grey and yellow sticks while the DNA is shown as light grey sticks. Water is portrayed as a light grey field. (Right) DNA chains and water molecules distribution within the architectures of the TEA-core DNA/*$\boldsymbol{G_6}$ *nanoscopic assembly. In this case, water is represented as a coloured density field: according to the scale reported in the lower left corners of the panels, blue density values are black, while high density values are white. Adapted with permission form Liu, X.X.; Wu, J.; Yammine, M.; Zhou, J.; Posocco, P.; Viel, S.; Liu, C.; Ziarelli, F.; Fermeglia, M.; Pricl, S.; Victorero, G.; Nguyen, C.; Erbacher, P.; Behr, J.P.; Peng, L. Structurally flexible triethanolamine core PAMAM dendrimers are effective nanovectors for DNA transfection in vitro and in vivo to the mouse thymus. Bioconjug. Chem., 2011, 22(12), 2461-2473. Copyright {2011} American Chemical Society.*

From a structure-activity relationship (SAR) standpoint, the enhanced swelling capacities of the TEA-core dendrimers at low pH values may result in a higher buffering capacity which, in turn, can be beneficial to endosomal escape of the nucleic acid cargo via the proton sponge effect. At the cellular level, in fact, inadequate cytosolic access is one major challenge that must be overcome if nanovector/DNA(RNA) systems are to become effective in vivo therapeutics. The increased swelling and, possibly, the increased proton sponge effect of more flexible and open structure dendrimers such as the TEA-core PAMAMs undoubtedly concur to enhance the capacity of these nanovectors and their cargoes to enter the endosome, adsorb protons, swell and cause an influx of negative (e.g., Cl^-) counterions which, in turn, creates an osmotic effect ultimately leading to water uptake. This escalation of events are purported to cause endosome membrane destabilization and rupture, with subsequent release of the nanodelivery complex in the cellular cytosol. Thus, should the proton sponge effect be the operative mechanism underlying endosome escape of the nanovector and release of it payload, then flexibility, softness, and conformational freedom are all key molecular parameters in a dendrimer-based nanocarrier.

5 DENDRIMERS AND DENDRONS AS MULTIVALENT NANOVECTORS

Multivalent systems are widely found in nature, and especially in biology: adhesion of viruses or bacteria to cells' surface, cell to cell adhesion, and cell to polyvalent molecule interactions. A good example of multivalency resides in the defence process of the immune system involving bacteria, antibodies, and macrophages. Antibodies have the ability to recognize non-self entities, such as bacteria, upon polyvalent binding with antigens, or other proteins, located at their surface. It is noteworthy that weak ligand-receptor

interactions can be made much stronger simply by the simultaneous bonding of these ligands to these multiple receptors.

High-affinity molecular recognition of biomolecular targets is of crucial importance in the development of synthetic systems capable of intervening in biological pathways; multivalent recognition is a key principle in enhancing binding strength and hence developing systems with potential biomedical applications. Experimental studies and mathematical models have demonstrated that once the first ligand in a multivalent array has bound to the target, the binding of a second ligand is usually a cooperative, entropically less disfavoured process, with a local concentration effect also enhancing binding.

Dendrimers and dendrons are inherent multivalent ligands that can present multiple recognition elements from a central scaffold. The scaffold plays a crucial role because it moulds the final architecture in term of shape, orientation of recognition elements, flexibility, size and valency. When the multiple surface groups are ligands, the dendritic scaffolding can be considered to act as a kind of nanoscaffolding, organizing the ligand array. As such, dendritic systems have been widely exploited for their potential applications in multivalent biological recognition. ,

Self-assembly is an incredibly powerful concept in modern molecular science. The ability of carefully designed building blocks to spontaneously assemble into complex nanostructures underpins developments in a wide range of technologies, from materials science to molecular biology. Self-assembly is a supramolecular approach which relies on complementary noncovalent interactions, such as electrostatic and van der Waals forces, hydrogen bonds, coordination interactions and solvophobic effects. In self-assembled structures, these temporal intermolecular forces connect to the molecular scale building blocks in a reversible, controllable, and specific way. Of particular value are the possibilities offered by self-assembly to generate nanoscale complexity with relatively little synthetic input. Furthermore, the ability of self-assembled superstructures to behave as more than the sum of their individual parts, and exhibit completely new types of behaviour, is of special interest and appealing in (bio)nanotechnology.

There are a number of different ways in which dendrimers or dendrons can be assembled in solution; perhaps the most efficient approach is the one that gives rise to well-defined (i.e., monodisperse) assemblies of dendritic building blocks. The supermolecular structures generated using this approach are generally based on well-established, specific intermolecular interactions; consequently, each assembly contains a defined number of dendritic building blocks. Such supermolecular dendrimeric structures have an equivalent degree of structural definition to a traditional covalent dendrimer; however, they are held together by reversible, nonbonded interactions. Given the relative simplicity of using self-assembly as a noncovalent synthetic tool, this approach is relatively cost-effective, and its potential for genuine future applications is therefore significantly enhanced.

Surface-active amphiphilic molecules are well-known to assemble into discrete structures such as micelles and vesicles in water solution. Amphiphilic dendritic systems are not exception to this rule, and a range of dendrimers with surfactant-like assembly properties have been reported. Indeed, when mixed with water, the apolar and polar regions of these Janus-type molecules will attempt to phase separate via self-assembly into structures such as micelles. Importantly, only in some cases does the aggregation process give rise to true micellar structures: this occurs at molecular concentrations C greater than the so-called critical micellar concentration (CMC), which is one of the key parameter in self-assembly. When C > CMC, aggregates with a variety of different, non-micellar structures – often ill-defined – are formed. In other words, CMC defines the

thermodynamic stability of the micelles. The latter is a very critical property in drug-delivery applications of micelles because intravenous injection of micellar solutions are associated with extreme dilutions by circulating blood (usually about 25-fold dilution at bolus injection or a much higher dilution at infusion). If the concentration of a micelle forming molecule in the circulation drops below the CMC, the micelles may be prematurely destroyed, resulting in the release of their cargo into the bloodstream before it reaches its target. This, in turn, will not only result in a poor therapeutic regime but, perhaps more importantly, could be dangerous because off-target and other unwanted side effects might (and likely will) originate. On the other hand, amphiphilic compound concentration cannot be increased above some critical values that correspond to the onset of micellar aggregation and precipitation, provoked by the interpenetration of the hydrophilic micellar coronas.

5.1 Aggregation of Amphiphilic Dendrons in Solution

Under the perspective outlined above, Smith's group recently synthesized a series of dendrons with a variety of lipophilic units at their focal points and tested these molecules for DNA binding and cell transfection capacities, revealing a set of stimulating evidences: not only all modified dendrons were able to tightly bind DNA and efficiently transfect cells, but for the first time and with the aid of multiscale molecular modeling a structure-activity relationship (SAR) could be formulated between the DNA binding affinity and the overall surface charge σ_m of the micellar assemblies but, perhaps more importantly, the SAR could be extended to cellular gene delivery, as σ_m plays a fundamental role in controlling the extent of the endosomal escape.[1(c)]

Thus, state-of-the-art multiscale simulation techniques were employed to monitor the dendrons self-assembly processes and to gain an insight into the types of aggregates eventually formed. First of all, the simulations revealed that all hydrophobically modified dendrons of generation 1 were able to form spherical supermolecular structures (see Figure 8) with diameters D_m in the range of 3 - 5 nm (see Table 3 and Scheme 3).

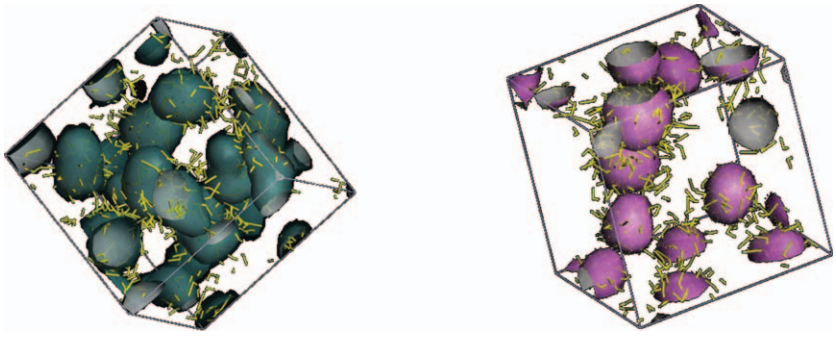

Figure 8 *Mesoscale modeling of amphiphilic dendrons showing aggregation into spherical micellar objects. In all pictures, the yellow sticks represent the dendron head groups while sea green and purple spheres are adopted to portray the various hydrophobic regions. Water and counterions are omitted for clarity. Adapted with permission from Jones, S.P.; Gabrielson, N.P.; Wong, C.H.; Chow, H.F.; Pack, D.W.; Posocco, P.; Fermeglia, M.; Pricl, S.; Smith, D.K. Hydrophobically modified dendrons: developing structure-activity relationships for DNA binding and gene transfection. Mol. Pharm.,* ***2011****, 8(2), 416-429. Copyright {2012} American Chemical Society.*

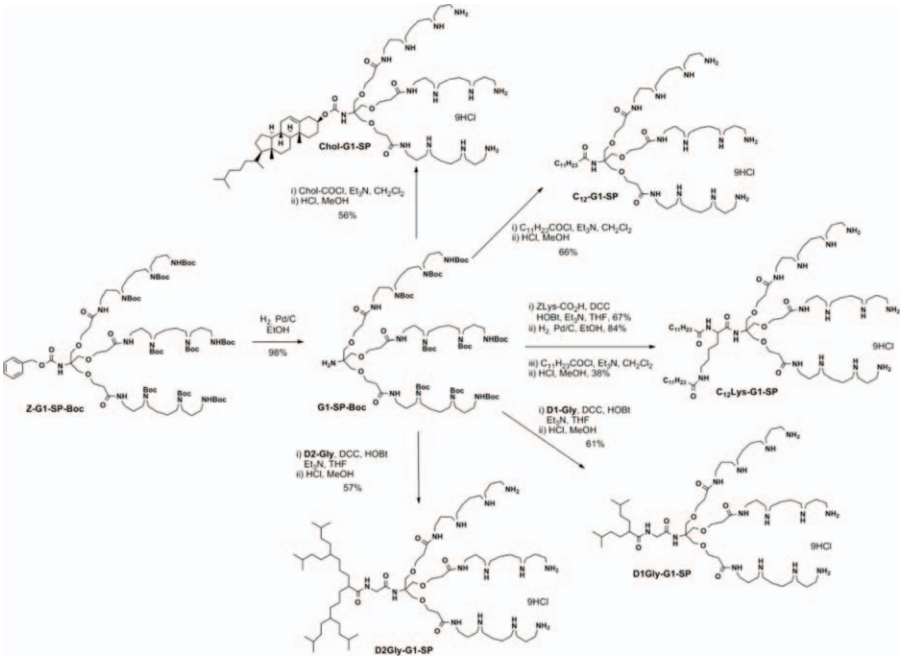

Scheme 3 *Chemical structures of the first generation dendron-based nanovectors with different hydrophobic groups at the focal point. Adapted with permission from Jones, S.P.; Gabrielson, N.P.; Wong, C.H.; Chow, H.F.; Pack, D.W.; Posocco, P.; Fermeglia, M.; Pricl, S.; Smith, D.K. Hydrophobically modified dendrons: developing structure-activity relationships for DNA binding and gene transfection. Mol. Pharm., 2011, 8(2), 416-429. Copyright {2012} American Chemical Society.*

Table 3 *Values of the micellar diameter D_m (nm), aggregation number N_{agg}, and micelle surface charge density σ_m (e/nm^2) for different amphiphilic dendrons as obtained from mesoscale simulations. Adapted with permission from Jones, S.P.; Gabrielson, N.P.; Wong, C.H.; Chow, H.F.; Pack, D.W.; Posocco, P.; Fermeglia, M.; Pricl, S.; Smith, D.K. Hydrophobically modified dendrons: developing structure-activity relationships for DNA binding and gene transfection. Mol. Pharm., **2011**, 8(2), 416-429. Copyright {2012} American Chemical Society.*

Compounds	D_m	N_{agg}	σ_m
Chol-G1-SP	3.4 ± 0.1	21	5.2
C_{12}Lys-G1-SP	4.0 ± 0.2	24	4.3
D2Gly-G1-SP	4.9 ± 0.2	32	3.8
C_{12}-G1-SP	4.0 ± 0.1	16	2.8
D1Gly-G1-SP	4.0 ± 0.2	12	2.1

The spherical geometry of the self-assembled supramolecular entities is a direct consequence of the conical molecular shape of each dendron, featuring a relative large cationic head and a comparatively small lipophilic part. In fact, assembly geometries for amphiphilic molecules is dictated by the proportions of their polar and apolar domains, aptly described by the so-called packing parameter $P = v_h/a_0l_c$,[16] in which v_h is the volume of the densely packed hydrophobic segment, a_0 is the effective cross-sectional area of the hydrophilic group, and l_c is the chain length of the hydrophobic moiety normal to the interface. Based on simple geometric considerations of micellar core volume *vs*. surface area, it is easy to show that $P < 1/3$ is characteristic of spherical micelles, $1/3 < P < 1/2$ characterizes self-assembly of cylindrical shape, $1/2 < P < 1$ corresponds to vesicles, flat lamellae are formed at P = 1 and, lastly, inverted micelles are expected for $P > 1$.

By coupling basic molecular modeling concepts to the dimensional micellar parameters estimated by mesoscopic simulations we were able to calculate the corresponding value of packing parameter *P* for all modified dendrons under hydrated conditions, which in all cases fell between 0.24 and 0.32, in agreement with the corresponding spherical morphologies predicted by our mesoscopic simulations.

5.2 Aggregation of Amphiphilic Dendrons in the Presence of a Nucleic Acid

Mesoscale simulations of the same dendron micelles carried out in the presence of DNA neatly showed that, in all cases, the overall systems consist of parts of free, unfolded, single-chain DNA that connect micelles on which a partial amount of DNA has been adsorbed (see Figure 9). In other words, all dendron/DNA complexes present a typical beads-on-a-string structure, made of dendron micelles connected by a DNA thread. Importantly, this predicted morphology is supported by detailed AFM studies between G4 PAMAM dendrimers and DNA – indicative that these self-assemblies of dendrons can be considered to be somewhat like covalently bound higher generation spherical dendrimers. These structures are also somewhat reminiscent of the structure of open chromatin, which consists of an array of nucleosome core particles, separated from each other by up to 80 base pairs of linker DNA. However, in clear contrast to the periodic structure of open chromatin, the dendron micelles appear to be distributed in a non-periodic, more irregular way.

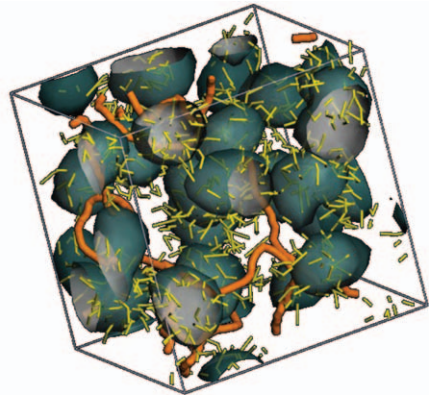

Figure 9 *Mesoscale modeling of the interaction of DNA with an amphiphilic dendron. In this Figure, yellow sticks represent dendron head groups, while coloured spheres are adopted to represent the hydrophobic region of the micelles. Water is omitted for clarity. DNA molecules are depicted as orange sticks. Adapted with permission from Jones, S.P.; Gabrielson, N.P.; Wong, C.H.; Chow, H.F.; Pack, D.W.; Posocco, P.; Fermeglia, M.; Pricl, S.; Smith, D.K. Hydrophobically modified dendrons: developing structure-activity relationships for DNA binding and gene transfection. Mol Pharm., 2011, 8(2), 416-429. Copyright {2012} American Chemical Society.*

5.3 Critical Micellar Concentration of amphiphilic dendrons

According to the classical laws of thermodynamics, the free energy of micellization ΔG_{mic} – i.e., the driving force that might eventually lead the amphiphilic molecules to spontaneously aggregate in water – can be expressed in the simple form $\Delta G_{mic} = -RTlnK_m$, where K_m is the equilibrium constant between the aggregated and free forms of the given amphiphile in the aqueous environment. For conditions near or above the CMC, it can be shown that the above expression for ΔG_{mic} can be approximated to the form $\Delta G_{mic} =$

RTln(CMC). Accordingly, once either ΔG_{mic} or CMC is known, the other parameter can be easily estimated through this simple, fundamental relationship.

Following the theory originally proposed by Tanford and subsequently modified by other authors, and using the information available from our multiscale simulations, we were able to calculate the values of ΔG_{mic} and the corresponding CMCs for the five modified dendrons of Table 3. Interestingly, ΔG_{mic} at room temperature has large, negative values, indicating that micellisation is a spontaneous and highly favourable process for all amphiphilic dendrons, although ΔG_{mic} decreases on going from Chol-G1-SP to D_1Gly-G1-SP (in the order: -87.56 kcal/mol and 0.021 μM; -80.42 kcal/mol and 0.089 μM; -77.97 kcal/mol and 0.15 μM; -55.92 kcal/mol and 12.5 μM; -49.29 kcal/mol and 47.6 μM, respectively). Since the head group architecture is the same in all amphiphiles, the main differential contribution to ΔG_{mic} must originate from differences in the size and structure of the hydrophobic component.

Typically, micellar aggregates have CMCs of the order of 10^{-3}-10^{-5} M, while lower CMCs, even down to the nanomolar range can be found for amphiphiles that form either membranes or cylindrical aggregates. Amphiphiles showing low CMCs tend to have relatively large hydrophobic segments, and this normally results in an assembly shape with a lower curvature. However, our series of modified dendrons combine a large hydrophobic portion with a very large head group, resulting in a roughly conical amphiphile. The size of the hydrophobic segment is responsible for the low CMCs, while the large size of the head group results in the spherical geometry of the assembly.

It is of particular interest to note that the predicted CMC values for C_{12}-G1-SP and D_1Gly-G1-SP lie above the concentrations of the DNA binding assays (i.e. low μm concentrations) – as such, it is possible that the relatively poor DNA binding ability of these compounds reflects the fact that they are not aggregated under the experimental conditions as a consequence of their relatively small hydrophobic segments. Although a word of caution is due about the fact that the calculated values of ΔG_{mic} and CMC are obtained using validated but simplified theoretical approaches, the trends exhibited by these parameters are in line with the experimental data. Indeed, we were able to carry out full experimental aggregation studies on a closely related set of hydrophobically modified dendrons, and for these systems, the in silico predictions of micelle diameters, charge densities and CMC values were closely mirrored by the experimental results, both in terms of trends and absolute values, thus strengthening not only the reliability of the entire computational procedure applied but, perhaps more importantly, validating its predictive capacity.

Figure 10 graphically recaps the major finding of the study summarized and discussed above in terms of a graphical perspective of the qualitative relationship between the main properties of the self-assembled dendron systems investigated and their performance as gene delivery nanovectors.

6 CONCLUSIONS

In conclusion, the extensive series of examples illustrated and discussed above - taken from our own experience in the field - emphasizes the role and potentiality of multiscale molecular modeling in the pre- and post-development of nanodevices for gene delivery. Accurate and reliable molecular modeling can be performed more easily than experiments. In silico evaluation can take into account the molecular specificity of the problem and dramatically reduce the time and cost required to formulate a new device and therapeutic intervention, and eventually translate it into the clinical setting. In nanomedicine, the need

for accurate multiscale molecular modeling is even more pressing. Despite its rapid growth and extraordinary potential, the field is still in its infancy, is highly interdisciplinary, and aims at solving problems of extraordinary and unprecedented complexity. With such a scenario, multiscale molecular modeling could afford a substantial contribution in dictating the success of nanomedicine and make the difference between several years of unfruitful research and the development of new, revolutionary therapeutic strategies readily available to the public.

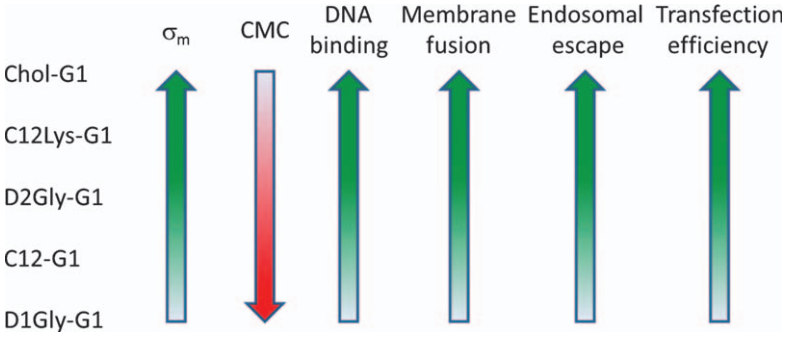

Figure 10 *Qualitative structure-activity relationship (SAR) of the main properties of the self-assembled dendron systems and their performance as gene delivery nanovectors. The green colour denotes a positive effect while the red colour a negative one. The direction of the arrow head indicates an increase (upward direction) or a decrease (downward direction) of the relevant property/performance.*

References

1 (a) P. Posocco, E. Laurini, V. Dal Col, D. Marson, K. Karatasos and S. Pricl, *Curr. Med. Chem*. 2012, **19**, 5062.; (b) A. Barnard, P. Posocco, S. Pricl, M. Calderon, R. Haag, M.E. Hwang, V.W. Shum, D.W. Pack and D. K. Smith, *J. Am. Chem. Soc*. 2011, **133**, 20288; (c) S.P. Jones; N.P. Gabrielson, C.H. Wong, H.F. Chow, D.W. Pack, P. Posocco, M. Fermeglia, S. Pricl and Smith, D.K., *Mol. Pharm*. 2011, **8**, 416; (d) P. Posocco, S. Pricl, S. P. Jones, A. Barnard and D. K. Smith, *Chem. Sci*. 2010, **1**, 393, and reference therein.

2 (a) P. Posocco, C. Gentilini, S. Bidoggia, A. Pace, P. Franchi, M. Lucarini, M. Fermeglia, S. Pricl and L. Paquato, *ACS Nano* 2012, **6**, 7243; (b) R. Toth, F. Santese, S.P. Pereira, D.R. Nieto, S. Pricl, M. Fermeglia and P. Posocco, *J. Mater. Chem*. 2012, **22**, 5398; (c) P. Posocco, M. Fermeglia and S. Pricl, *J. Mater. Chem*. 2010, **20**, 7742, and references therein.

3 (a) K. Ciepluch, N. Katir, A. El Kadib, A. Felczak, K. Zawadzka, M. Weber, B. Klajnert, K. Lisowska, A.M. Caminade, M. Bousmina, M. Bryszewska and J.-P. Majoral, *Mol. Pharm*. 2012, **9**, 458; (b) K. Milowska, J. Grochowina, N. Katir, A. El Kadib, J.-P. Majoral, M. Bryszewska and T. Gabryelak, *J. Lumin*. 2012, article asap http://dx.doi.org/10.1016/j.jlumin.2012.08.060.

4 D. Marson, P. Posocco, E. Laurini, M. Fermeglia, K. Ciepluch, B. Klajnert, M. Bryszewska, N. Katir, A. El Kadib, A.-M. Caminade, J.-P. Majoral and S. Pricl, manuscript in preparation.

5 S. Asaftei and E. De Clercq, *J. Med. Chem*. 2010, 53, 3480.

6 A.-M. Caminade, C.-O, Turrin and J.-P. Majoral, *New J. Chem*. 2010, **34**, 1512.

7 J. H. Zhou, J. Y. Wu, N. Hafdi, J.-P. Behr, P. Erbacher and L. Peng, *Chem. Commun*. 2006, 2362.
8 X. Liu, P. Rocchi, F. Q. Qu, S. Q. Zheng, Z. C. Liang, M. Gleave, J. Iovanna and L. Peng, *ChemMedChem* 2009, **4**, 1302.
9 X. Liu, J. Wu, M. Yammine, J. Zhou, P. Posocco, S. Viel, C. Liu, F. Ziarelli, M. Fermeglia, S. Pricl, G. Victorero, C. Nguyen, P. Erbacher, J.P. Behr and L. Peng, *Bioconjug. Chem*. 2011, **22**, 2461.
10 K. Karatasos, P. Posocco, E. Laurini and S. Pricl, *Macromol. Biosci*. 2012, **12**, 225.
11 G.M. Pavan, P. Posocco, A. Tagliabue, M. Maly, A. Malek, A. Danani, E. Ragg, C.V. Catapano and S. Pricl, *Chemistry Eur. J*. 2010, **16**, 7781.
12 (a) S.P. Jones, G.M. Pavan, A. Danani, S. Pricl and D.K. Smith, *Chemistry Eur. J*. 2010, **16**, 4519; (b) G.M. Pavan, A. Danani, S. Pricl and D.K. Smith, *J. Am. Chem. Soc*. 2009, **131**, 9686.
13 J. Zhou, C.P. Neff, X. Liu, J. Zhang, H. Li, D.D. Smith, P. Swiderski, T. Aboellail, Y. Huang, Q. Du, Z. Liang, L. Peng, R. Akkina and J.J. Rossi, *Mol. Ther*. 2011, **19**, 2228.
14 A.L. Bolcato-Bellemin, M.E. Bonnet, G. Creusat, P. Erbacher and J.P. Behr, *Proc. Natl. Acad. Sci. U.S.A*. 2007, **104**, 16050.
15 X. Liu, C. Liu, E. Laurini, P. Posocco, S. Pricl, F. Qu, P. Rocchi and L. Peng, *Mol Pharm*. 2012, **9**, 470.
16 (a) J.N. Israelachvili, D.J. Mitchell and B.W. Ninham, *Biochim. Biophys. Acta, Biomembr.* 1977, **470**, 185; b) J.N. Israelachvili, D.J. Mitchell and B.W. Ninham. *J. Chem. Soc., Faraday Trans. II* 1976, **72**, 1525.

Subject index